Preprints (www.preprints.org) | NOT PEER-REVIEWED | Posted: 2 June 2021 doi:10.20944/preprints202106.0062.v1

Assessment of Snowfall Accumulation from Satellite and Reanalysis Products using SNOTEL Observations in Alaska

Yang Song, Patrick D. Broxton, Mohammad Reza Ehsani, Ali Behrangi

The University of Arizona, Department of Hydrology and Atmospheric Sciences

Corresponding author: Ali Behrangi, behrangi@email.arizona.edu

Abstract

The combination of snowfall, snow water equivalent (SWE), and precipitation rate measurements from 39 Snow Telemetry (SNOTEL) sites in Alaska are used to assess the performance of various precipitation products from satellites, reanalysis, and rain gauges. Observation of precipitation from two water years (2018-2019) of the high resolution radar/rain gauge data (Stage IV) product was also utilized to add insights into scaling differences between various products. The outcomes were also used to assess two popular methods for rain gauge undercatch correction. It was found that SWE and precipitation measurements at SNOTELs, as well as precipitation estimates based on Stage IV data, are generally consistent and can provide a range in which other products can be assessed. Time-series of snowfall and SWE accumulation suggests that most of the products can capture snowfall events; however, differences exist in their accumulation. Reanalysis products tend to overestimate snow accumulation in the study area, while current combined passive microwave remote sensing products (i.e., IMERG-HQ) underestimate snowfall accumulation. We found that corrections factors applied to rain gauges are effective in improving their undercatch, especially for snowfall. However, no improvement in correlation is seen when correction factors are applied, and rainfall is still estimated better than snowfall. Even though IMERG-HQ has less skill in capturing snowfall than rainfall, analysis using Taylor plots showed that the combined microwave product does have skill in capturing the geographical distribution of snowfall and precipitation accumulation, so bias adjustment might lead to reasonable precipitation estimates. This study demonstrates that other snow properties (e.g., SWE accumulation at the SNOTEL sites) can complement precipitation data to estimate snowfall. In the future, gridded SWE and snow depth data from GlobSnow and Sentinel-1 can be used to assess snowfall and its distribution over broader regions.

Keywords: Alaska; SNOTEL; Snowfall accumulation; IMERG; precipitation

© 2021 by the author(s). Distributed under a Creative Commons CC BY license.

Preprints (www.preprints.org) | NOT PEER-REVIEWED | Posted: 2 June 2021 doi:10.20944/preprints202106.0062.v1

Introduction

Accurate quantitative knowledge of the amount and distribution of precipitation, precipitation phase, and snowpack is important for global water cycle studies, hydrology, and water resource management. For example, rainfall and snowfall affect streamflow differently, as streamflow response to rainfall is almost immediate while streamflow response to snowfall can be delayed many months. In contrast to rainfall, snowfall can be accumulated as snowpack and can act as a natural reservoir, storing water in mountains and cold regions and form an important water resource for warmer seasons. Accurate estimations of rainfall, snowfall, and snowpack amount and distribution are thus important. While snowmelt remains as a critical source of freshwater for the world population (Barnett et al., 2005; Arabzade et al. 2020), in a warming climate, snowpack amounts are being reduced (Kunkel et al., 2016; Zeng et al., 2018) and most of the precipitation may fall as rain instead of snow. However, snowfall is still the dominant form of precipitation in high latitudes (Behrangi, Stephens, et al., 2014; Levizzani et al., 2011; Liu, 2008).

Snowfall is most accurately measured using in-situ observations. However, these in-situ data are sparse in high latitudes and snow dominated regions (including mountains), partly due to the expense and difficulty of their installation and maintenance. Rain gauges are often used as ground truth for precipitation measurements, but they are not typically designed for snowfall measurement and they often face snowfall undercatch issue and may not be well maintained. Correction factors (CFs) are applied to correct for the underestimation of precipitation. CFs are often much larger and more uncertain for snowfall than rainfall and can be up to a factor of 3 in many regions (Fuchs et al., 2001; Goodison et al., 1998; Legates & Willmott, 1990; D. Yang et al., 2001).

Satellite data make it possible to estimate precipitation rate from space, with almost global coverage. However, the quality of precipitation retrieval, especially snowfall, from most of the satellites is relatively poor (e.g., Behrangi, Andreadis, et al., 2014; Behrangi, Tian, et al., 2014). The problem is larger in high latitudes where light rain and snowfall produce weak signals to be captured by sensors. Furthermore, the dynamic nature of surface emissivity over snow and ice surfaces makes it challenging to retrieve precipitation from passive microwave (PMW) sensors that are key to the Global Precipitation Measurement (GPM) mission (Skofronick-Jackson et al., 2017). As a result, for example, the Integrated Multi-Satellite Retrievals for GPM (IMERG) product (Huffman et al., 2020) uses geostationary infrared for precipitation retrieval within 60° N/S, but poleward of this region where geostationary images are too oblique, no estimate from the satellite is provided. In lack of quality PMW precipitation estimates in high latitudes, the Global Precipitation Climatology Project (GPCP) (Adler et al., 2017; Huffman et al., 2020) uses precipitation retrieval from the Atmospheric Infrared Sounder (AIRS; Susskind et al., 1997), although the relationship between infrared data and precipitation is not physically robust. To refine merged products, more efforts are needed to evaluate and compare the performance of the new generation of PMW precipitation products with AIRS and other infrared sensors in high latitudes (Adhikari et al., 2020; Ehsani et al., 2021). However, performing this important task is difficult due to the limited availability of quality in-situ observations in high latitude regions.

In the cold season, many regions experience subfreezing temperatures for several days or months. Snowfall is accumulated during these periods, and snowmelt is negligible. This can create an

Preprints (www.preprints.org) | NOT PEER-REVIEWED | Posted: 2 June 2021 doi:10.20944/preprints202106.0062.v1

opportunity to investigate other aspects of snow that can potentially help assess snowfall amount. For example, by using mass property of snow, it is possible to use changes in snow mass to estimate snowfall accumulation within a certain accumulation period. Using the observation of mass change from the Gravity Recovery and Climate Experiment (GRACE), Behrangi et al. (2018a) calculated snowfall accumulation over cold regions in the northern hemisphere and used the values to assess two popular gauge-undercatch correction factors (CFs): Legates climatology (CF-L) utilized in GPCP, and Fuchs dynamic correction model (CF-F) used in the Global Precipitation Climatology Centre (GPCC) monitoring product (Schneider et al., 2017). The difference between the two CFs can exceed 50% (Behrangi et al., 2018a, 2019), so selection of the more accurate CF is important. Their results show a greater consistency between GRACE-based snow accumulation estimate and GPCC-F (GPCC corrected by CF-F) than GPCC-L (GPCC corrected by CF-L), in terms of both amount and spatial pattern of snowfall accumulation over the studied regions. However, GRACE offers a relatively coarse temporal (i.e., about a month) and spatial (about 300 km) resolution that limits its application in several places. Furthermore, the application of GRACE over mountainous regions and glaciers is complicated due to the coarse resolution and issues related to ice age rebound and glacier dynamics (Larsen et al., 2004).

Another approach could be to use observation of snow water equivalent (SWE) because, during the snow accumulation period, SWE and snowfall are well connected (Broxton et al., 2016a). Therefore, high quality observations of SWE can be valuable to assess snowfall. Behrangi et al. (2018b) utilized SWE estimates from the Airborne Snow Observatory (ASO) (Painter et al., 2016) over two mountainous basins in California, and Panahi and Behrangi (2019) used SWE values from the University of Arizona SWE product (UA-SWE) (Broxton et al., 2016b; Zeng et al., 2018) over the northern CONUS to assess snowfall products. Gonzalez and Kummerow (2020) also used estimates of snowfall and SWE from the Advanced Microwave Scanning Radiometer (AMSR-E) instrument to assess the consistency in the snow products. However, due to large errors and shortcomings in the retrieval of both SWE and snowfall from AMSR-E, neither of these products were found to be effective in the assessment of the other one.

In this work, we use in-situ measurements of SWE and snowfall at SNOTEL stations in Alaska to assess a variety of remotely sensed, gauge-based, and reanalysis precipitation products, focusing on their ability to represent snowfall accumulation and distribution. Most of the study area is located north of 60°N where estimation of snowfall, in particular, is uncertain (Huffman et al., 2020), so this assessment provides valuable information about the type of products that yield the best results. In particular, this study allows us to assess different product types (gauge based, satellite, or reanalysis), different satellite measurement types (passive microwave vs infrared), and different undercatch correction factors applied to the gauge data (Fuchs or Legates). Furthermore, we assess the consistency of snowfall and SWE data, as well as the impact of spatial scaling between the in-situ observations and the coarse resolution precipitation products using relatively high resolution (4 km) precipitation estimates from the National Centers for Environmental Prediction (NCEP), rescaled to multiple resolutions.

Data and Method

The datasets used in this study are as follows:

Preprints (www.preprints.org) | NOT PEER-REVIEWED | Posted: 2 June 2021 doi:10.20944/preprints202106.0062.v1

(a) SNOTEL network is an automated system that collects real-time in-situ snowpack and other climatic data in the western U.S. and Alaska since 1981. Most SNOTEL stations provide daily and hourly measurements of snow water equivalent, precipitation, snow depth, air temperature, and sometimes other quantities such as wind speed, relative humidity and soil moisture. In this study, we use SWE measurements using snow pillows (hereafter referred to as SNOTEL-SWE) and precipitation measurements using precipitation gauges (hereafter referred to as SNOTEL-PG). The locations of SNOTELs used in this study are shown in Figure 1. The data can be retrieved from the government website of United States Department of Agriculture: https://www.nrcs.usda.gov/wps/portal/wcc/home/snowClimateMonitoring/snowpack/

(b) NCEP Stage IV is a gridded precipitation product based on the NEXRAD Precipitation Processing System and manual quality control at the River Forecast Centers in CONUS. It is available on local 4 km polar-stereographic grids at hourly, 6-hourly and 24-hourly (accumulated from the 6-hourly) resolutions (Nelson et al., 2016). The data availability is from December 2001 to February 2021, and it includes Alaska and Puerto Rico stations since April 2017 (https://data.eol.ucar.edu/dataset/21.093) at 6-hourly and daily scales.

(c) GPCC is a gridded-precipitation product over global land excluding Antarctica that interpolates station data from different rain gauge networks (Becker et al., 2013). GPCC contains various products. Here we used two: (1) the latest Full Data Daily product (version 2020) that uses an enhanced quality control and interpolation scheme and the maximum number of available gauges (referred to here as GPCC), and (2) the monitoring product version 2020 that provides monthly values based on CF-F. Both products are available at 1°x1° resolution from 1982 to 2019 and can be obtained from: https://opendata.dwd.de/climate_environment/GPCC/html/download_gate.html. Two variations of GPCC are also produced in this study to assess which CF is more effective: GPCC-F that is obtained by applying CF-F from the monitoring product to GPCC Full data, and GPCC-L that uses CF-L (based on Legates and Willmott 1990) to correct GPCC. Note that GPCC does not use SNOTEL data, and so the GPCC and SNOTEL data are largely independent of each other.

(d) GPCP is a widely used precipitation climatology product (Adler et al., 2003; Huffman et al., 2009) that utilizes precipitation estimates from both satellite and rain gauge data (through the GPCC product) after applying a gauge undercatch correction factor (CF-L). The latest version of the One-Degree Daily (1DD) product (GPCP V1.3) (Adler et al., 2017) is used in this study and is available since 1996. GPCP's satellite precipitation estimates over land and ocean come from several space-borne sensors, but in high latitudes and near the poles is mainly from IR sounders (Huffman et al., 2001), specifically the Atmospheric Infrared Sounder (AIRS) after 2003. GPCP 1DD V1.3 can be obtained from http://eagle1.umd.edu/GPCP_CDR/.

(e) AIRS is a hyperspectral resolution IR spectrometer on board the AQUA satellite and has been operational since 2002 (Aumann et al., 2003). The precipitation estimates from AIRS are based on the Susskind et al. (1997) algorithm and is available at 1° x 1° spatial grid at daily scale and can be retrieved from GES-DISC through https://disc.gsfc.nasa.gov/datasets/AIRS3SPD_7.0/summary.

(f) The Integrated Multi-satellitE Retrievals for GPM High Quality data (IMERG-HQ) provides a blend of inter-calibrated passive microwave estimates at 0.1° × 0.1° spatial

Preprints (www.preprints.org) | NOT PEER-REVIEWED | Posted: 2 June 2021 doi:10.20944/preprints202106.0062.v1

and half-hour temporal resolutions with global coverage since 2000 (Huffman et al., 2020). Here, the latest version of IMERG-HQ (Version 6) daily precipitation is used. The product is available from GES-DISC through: https://disc.gsfc.nasa.gov/datasets/GPM_3IMERGDF_06/summary?keywords=imerg%20v06.

(g) The Modern-Era Retrospective Analysis for Research and Applications, Version 2 (MERRA2) is a popular reanalysis product that is available since 1980 at 0.5° × 0.625° and hourly resolution. MERRA2 substitutes the previous MERRA reanalysis with an upgraded data assimilation system to assimilate observations for the retrospective analyses (Gelaro et al., 2017). Here we used MERRA2 precipitation rate. The product can be obtained from the Goddard Earth Sciences Data and Information Services Center (GES DISC, https://disc.gsfc.nasa.gov/) and at https://disc.gsfc.nasa.gov/datasets?keywords=M2T1NXFLX.5.12.4&page=1.

(h) ERA5 is the fifth generation ECMWF atmospheric reanalysis product that uses the 4D-Var data assimilation technique (Hersbach, 2016) and is widely used by the community. ERA5 provides various meteorological parameters near the surface (in addition to multiple levels in the atmosphere) at relatively high resolution (e.g., 0.25°x0.25°, hourly back to 1979). Here we used precipitation rate, 2m air temperature, and sublimation from ERA5. The ERA5 products can be obtained from https://www.ecmwf.int/en/research/climate-reanalysis.

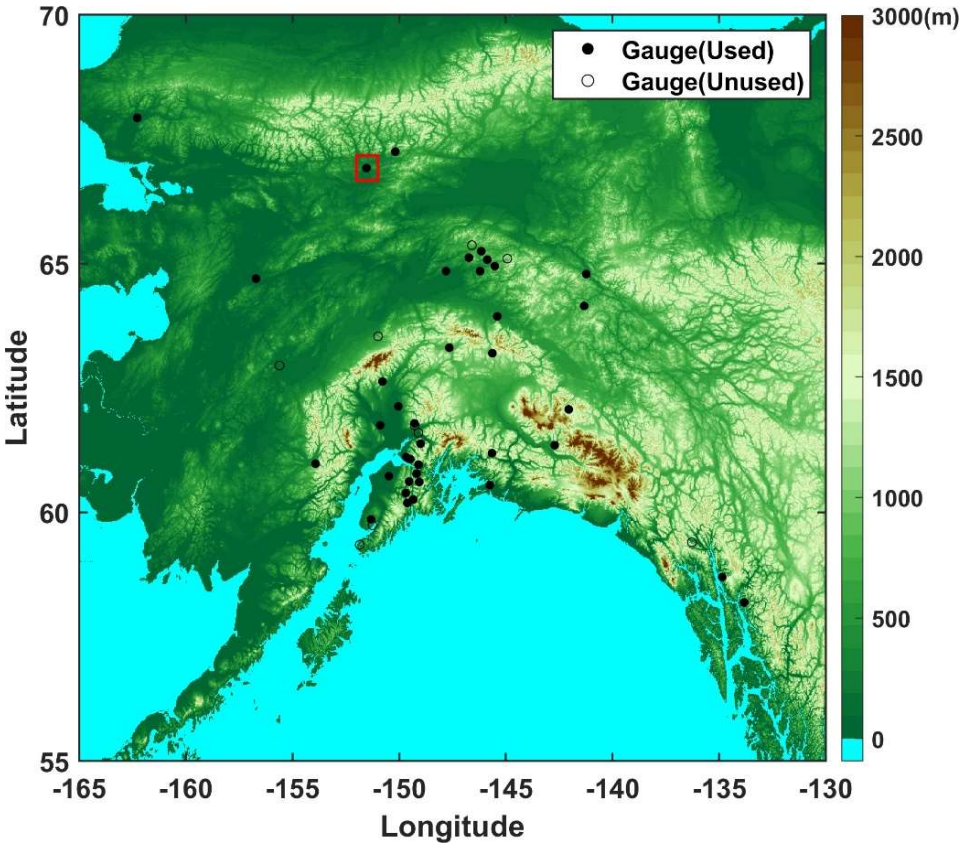

Figure 1. Location of SNOTEL stations used in this study with the topography map in the background. The empty circles represent the location of SNOTEL stations not used, mainly due to an incomplete record.

Preprints (www.preprints.org) | NOT PEER-REVIEWED | Posted: 2 June 2021 doi:10.20944/preprints202106.0062.v1

All the gridded products were mapped onto a common daily 1°x1° resolution grid, consistent with the resolution of GPCP and GPCC. For grids that contain a SNOTEL site, the gridded data were compared to the SNOTEL-SWE and SNOTEL-PG measurements. For the assessment of snowfall, this analysis was limited to the snow accumulation period when surface air temperature was continuously less than 0°C, ensuring that all SNOTEL-PG measurements were of snowfall and snow accumulation based on SNOTEL-SWE could be used as a surrogate for snowfall. In addition, to the SNOTEL data, we also used the NCEP stage IV product as an additional reference to add insight into the scaling differences between the in-situ SNOTEL data and the remote-sensing precipitation products. The study period covers 2017-2019 when Stage-IV data is available.

Results:

Error! Reference source not found. shows cumulative time-series of daily precipitation and snowfall (**Error! Reference source not found.**) along with the corresponding surface air temperature (T2m) (**Error! Reference source not found.**) at one of the SNOTEL stations (shown in Figure *1* with a red box) for water year 2018 (October 2017-September 2018). The arrow shows the location of peak SWE. Precipitation is accumulated from the start to the end of the water year, but snowfall is only accumulated between when T2m goes below 0 °C and when T2m goes above 0°C or peak SWE, whichever comes earlier (note in Figure 2 that snowfall is not accumulated for any product after the time of peak SWE). Because sublimation tends to be small in cold regions (i.e., as noted earlier, generally less than 3% of total precipitation accumulation during winter based on ERA-5 reanalysis data; also demonstrated in Behrangi et al. (2018a)), precipitation and snow accumulation plots should be fairly comparable during the accumulation phase. Outside of this accumulation phase, precipitation often occurs as rainfall and generally has higher accumulation slope than when all precipitation is snowfall (**Error! Reference source not found.**). **Error! Reference source not found.** suggests a few interesting points: (1) Almost all of the precipitation products (except for IMERG-HQ) capture major snowfall events (large positive increments in the accumulation plot), (2) IMERG-HQ tends to miss (or significantly underestimate) snowfall events, and its snowfall accumulation is very low (i.e., much smaller than the range identified by all of the other products), but it is more capable of capturing rainfall, (3) AIRS provides reasonable estimates of snowfall accumulation, but tends to overestimate precipitation accumulation toward the end of the water year, (4) SNOTEL-SWE and snowfall accumulation measured at the SNOTEL precipitation gauge (SNOTEL-PG) give comparable estimates of snow accumulation, though SNOTEL-SWE gives slightly higher estimates than SNOTEL-PG (that might be due to minor gauge undercatch for SNOTEL-PG or slight overestimation by SNOTEL-SWE at this site), (5) At peak SWE, GPCC-L and GPCC-F (i.e., GPCC after applying gauge undercatch correction factors CF-L and CF-F, respectively) are closest to SNOTEL-SWE, followed by GPCP. GPCC without CFs produces the lowest accumulation among all of the products, except IMERG-HQ, (6) Most products (except for GPCC, IMERG-HQ, MERRA2, and ERA5) fall inside the snowfall accumulation range determined by SNOTEL-SWE and SNOTEL-PG, and (7) At the end of the water year, AIRS shows higher precipitation accumulation than the rest of the products and IMERG-HQ, followed by GPCC (with no correction) show the least precipitation accumulation.

Preprints (www.preprints.org) | NOT PEER-REVIEWED | Posted: 2 June 2021 doi:10.20944/preprints202106.0062.v1

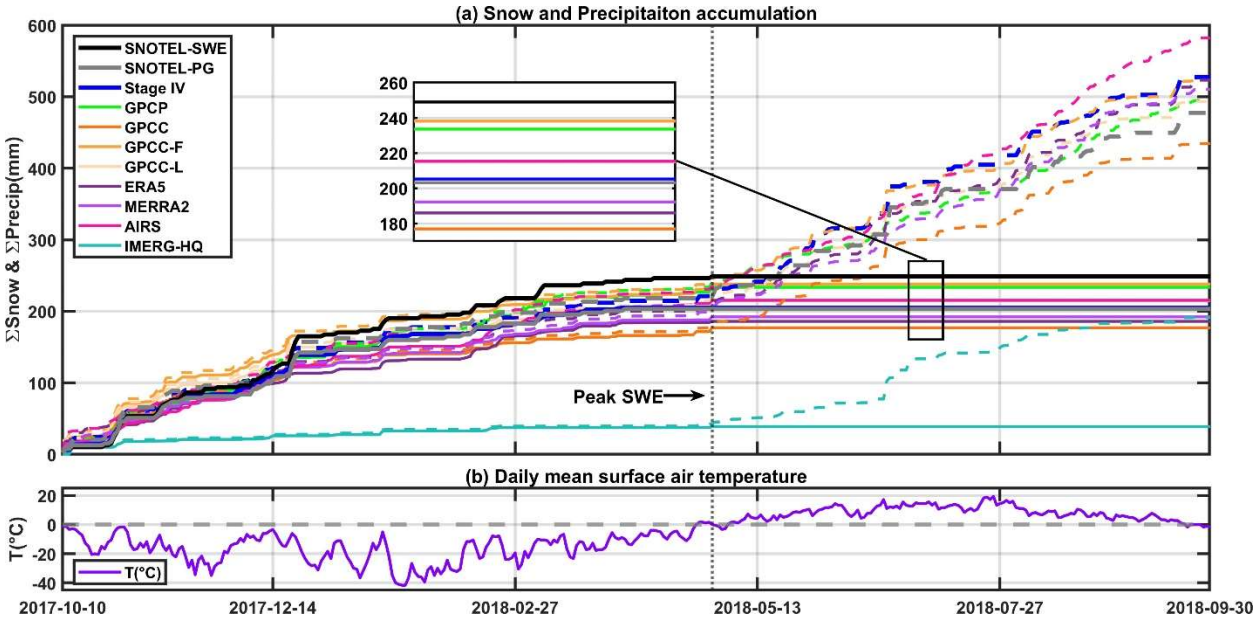

Figure 2. Cumulative time-series of (a) daily precipitation and SNOTEL-SWE together with the corresponding (b) surface air temperature (T2m) at one of the SNOTEL stations (shown in Figure 1 with a red box) for water year 2018.

Figure 3 shows mean (empty circles), median (the red line), as well as the 25th and the 75th percentile (boxes) of snowfall accumulation (prior to peak SWE and when T2m < 0^{o}C; Figure 3a), water year precipitation accumulation (Figure 3b), and their ratio (Figure *3*) for two water years (2018 and 2019). The 5th and the 95th percentile range are also shown with black dashed lines (extended from the boxes). Two versions of the Stage IV estimates are plotted: (1) the original 4 km resolution (Stage IV - 4 km), and (2) 1^{o}x1^{o} resolution (Stage IV - 1 deg), consistent with other products, in order to provide insight into the spatial scale difference that exists between SNOTEL and the gridded products. Similar to what is shown in Figure 2, SNOTEL-PG is fairly consistent with SNOTEL-SWE in terms of snowfall accumulation across all sites (Figure 3a). GPCC-F, GPCC-L, AIRS, and Stage IV products fall within the range identified by either mean or median of SNOTEL-PG and SNOTEL-SWE. The Stage IV products produce almost identical mean and median snowfall accumulation, but Stage IV – 4 km shows a larger range. They are also fairly consistent with the SNOTEL data (both SNOTEL-SWE and SNOTEL-PG). ERA5 shows the largest and IMERG-HQ shows the smallest snowfall accumulation among the products. For total precipitation at the end of water year (Figure *3*), Stage IV products, GPCP, GPCC-F-, GPCC-L and AIRS show the closest values to SNOTEL-PG both in terms of median and mean values. ERA5 and MERRA2 tend to overestimate both snowfall and precipitation accumulation, while GPCC and IMERG-HQ tend to underestimate snowfall and precipitation accumulation. With respect to the ratio of snow accumulation over total precipitation (Figure *3*), GPCP has the highest mean and median ratios and ERA5 and especially IMERG-HQ have the lowest ratios compared to

Preprints (www.preprints.org) | NOT PEER-REVIEWED | Posted: 2 June 2021 doi:10.20944/preprints202106.0062.v1

SNOTEL-PG. Similar to what is shown in Figure 2, this demonstrates that IMERG-HQ has less skill in capturing snowfall than rainfall.

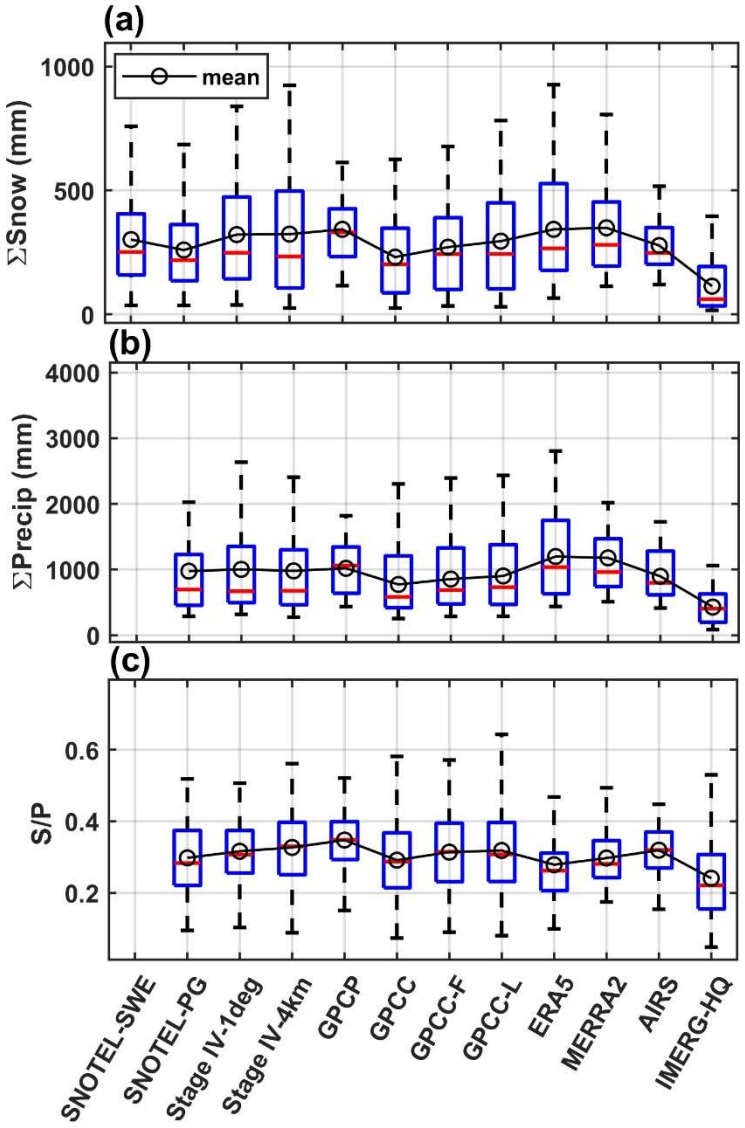

Figure 3. Comparison of the mean (empty circles), median (red line), 25th and 75th percentiles of (a) snowfall during the accumulation phase, (b) water year total precipitation, and (c) their ratio using two water years (2018 and 2019).

Figure *4* shows Taylor plots with SNOTEL-SWE and SNOTEL-PG as reference for snowfall accumulation (Figure *4* and Figure *4*) and SNOTEL-PG as reference for precipitation accumulation (Figure *4*). For snowfall accumulation, Figure *4* and Figure *4* suggest: (1) The choice of SNOTEL-SWE or SNOTEL-PG does not change the results, as the two products are very similar (e.g., the correlation coefficient (CC) is about 0.97 when compared against each other; Figure *4* and Figure *4*), (2) The Stage IV 4 km product has the highest CC (~ 0.85) for snow accumulation, followed by GPCC products, MERRA2, and Stage IV-1deg, which all show CC around 0.7, (3)

Preprints (www.preprints.org) | NOT PEER-REVIEWED | Posted: 2 June 2021 doi:10.20944/preprints202106.0062.v1

While correction factors are effective to reduce GPCC bias for snowfall accumulation (Figure *3*), GPCC-F and GPCC-L show slightly lower CC than GPCC; GPCC-F also outperforms GPCC-L with respect to standard deviation and root mean square error (RMSE), (4) GPCP shows slightly lower CC (~0.6) than GPCC products, probably because GPCP uses a combination of AIRS (CC ~0.5) and GPCC-L (CC ~0.7). ERA-5 also has CC ~0.6, and (5) While IMERG-HQ shows large underestimation of snowfall accumulation (Figure *3*), its CC (~0.6) and RMSE are within the range of other products, suggesting that IMERG-HQ has skill in capturing the snowfall accumulation patterns, and bias correction can improve IMERG-HQ.

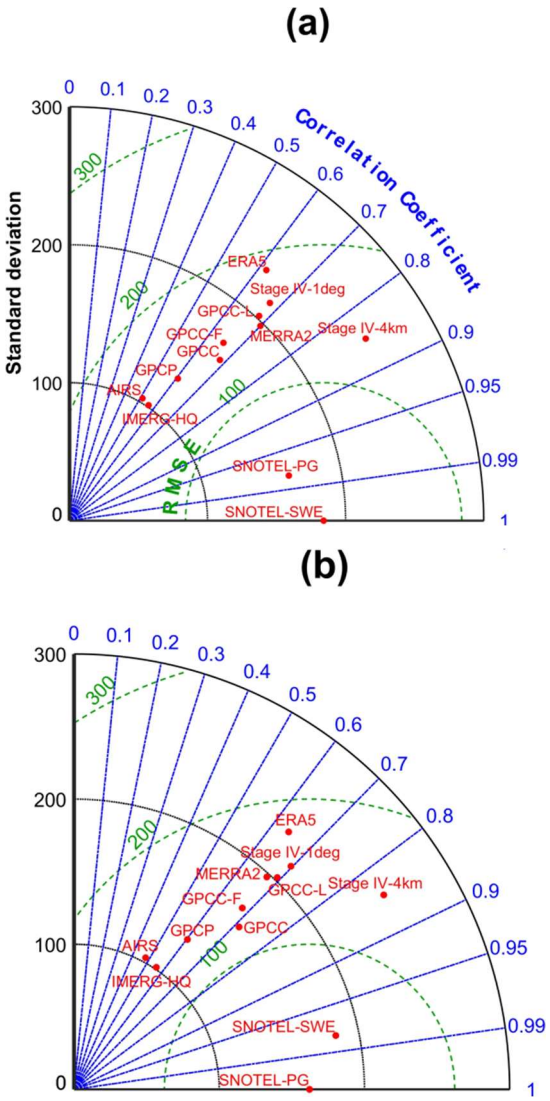

Preprints (www.preprints.org) | NOT PEER-REVIEWED | Posted: 2 June 2021 doi:10.20944/preprints202106.0062.v1

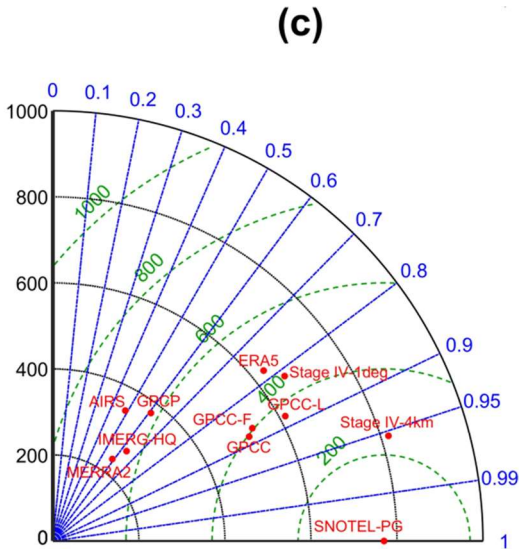

Figure 4. Taylor plots for snow accumulation with (a) SNOTEL-SWE and (b) SNOTEL-PG as references respectively, and (c) SNOTEL-PG as reference for precipitation accumulation.

For precipitation comparison, Figure *4* suggests: (1) most of the products show equal or better CC for precipitation than snowfall accumulation, (2) Stage IV-4 km shows the best CC (~0.95), followed by GPCC products and Stage IV-1 deg (which have CC between 0.8 and 0.9), (3) Unlike for snowfall accumulation, where MERRA outperforms ERA5, for precipitation accumulation, ERA5 has higher CC (~0.8), closer standard deviation to that of SNOTEL-PG, and lower RMSE compared to MERRA2, and (4) IMERG-HQ's CC (~0.6) is comparable to that of MERRA2 and GPCP, but GPCP shows better skill than IMERG-HQ and MERRA2 in terms of standard deviation and RMSE (Figure *4*).

SNOTEL-SWE, SNOTEL-PG and Stage IV observations are fairly consistent, even considering scale differences between the in-situ SNOTEL data and the gridded Stage IV data (see Figures 2 and 3), which suggests that they can be used to define 'observational' ranges for snowfall and precipitation accumulation (although SNOTEL-SWE can only be used to estimate snowfall). Figure *5* shows, at each SNOTEL station, which products fall within these observational ranges of snowfall (Figure *5*) and precipitation (Figure *5*) accumulation. Products that fall within these observational ranges are shown in white, while blue and red indicate which products under- or over-estimate snowfall and precipitation, with lighter (darker) colors showing closer (farther) distances to the observational ranges. For example, in Figure *5*, for station 951, GPCC-F and ERA5 fall within the observational range, GPCC, GPCC-L, and IMERG-HQ are below the observational range (with IMERG-HQ being farthest from the range), and GPCP, AIRS, and MERRA2 are above the observational range (with MERRA2 being farthest from the range). Numbers on the right-side of the plots show, for each product, the number of cases that are within the observational range. Figure *5*a shows that for snow accumulation, ERA5, MERRA2, GPCC-F, and GPCC-L have the highest number of 'hits' (white grids) inside the observational snow accumulation range, and IMERG-HQ has the least number of hits. For precipitation accumulation, GPCC-F has the highest number of hits followed by ERA5 and MERRA2. Figure *5* also shows that GPCP, ERA5, MERRA2, and AIRS tend to overestimate snowfall and precipitation

Preprints (www.preprints.org) | NOT PEER-REVIEWED | Posted: 2 June 2021 doi:10.20944/preprints202106.0062.v1

accumulation at most sites, while IMERG-HQ and GPCC tend to underestimate snowfall and precipitation accumulation, as can be seen by dominant red and blue grids in their corresponding rows.

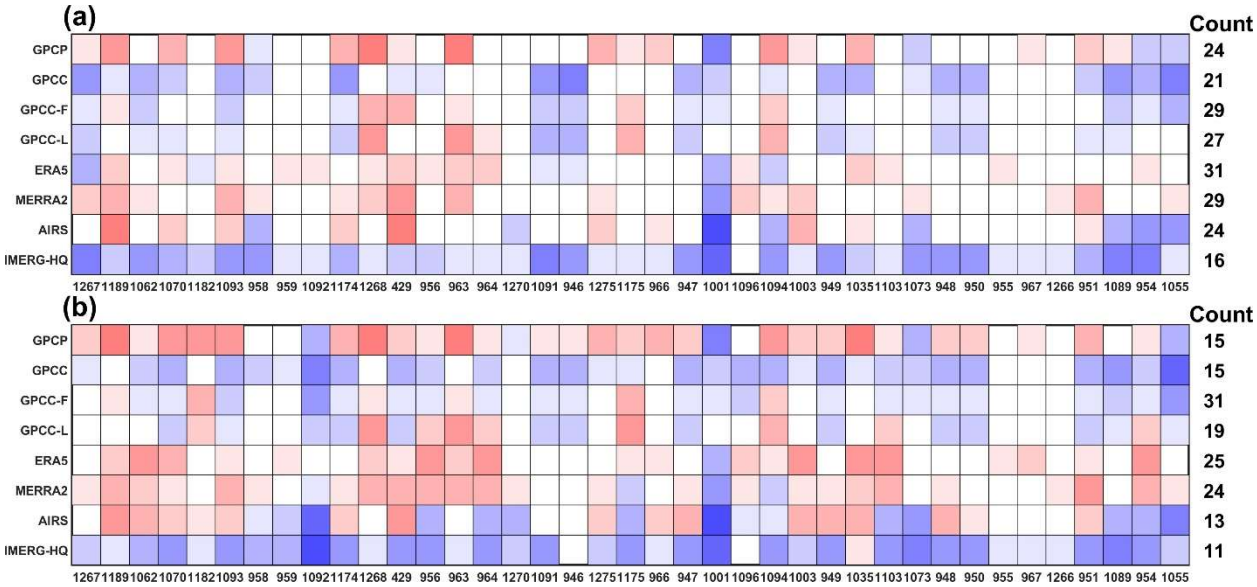

Figure 5. Comparison of snowfall and precipitation accumulation with the range defined by SNOTEL-PG, SNOTEL-SWE, and Stage IV for (a) snow accumulation and (b) precipitation accumulation at each SNOTEL site for water years 2018 and 2019. Numbers on the right sides of the plots indicate how often each product's snowfall or precipitation falls within the observational range.

Discussion

The analysis of SWE and snowfall accumulation at SNOTEL sites (SNOTEL-SWE and SNOTEL-PG) provide complementary information that adds valuable insights about the range of snowfall accumulation, as both measurements can be uncertain. Snowfall, measured using precipitation gauges, can be underestimated due to undercatch issues, and SWE accumulation can be affected by melting or sublimation, though they are often small during the snow accumulation phase in Alaska. We showed that the two estimates are also consistent with the corresponding values observed from Stage IV products at different scales. Together, these observational data can be used to assess several other precipitation products in Alaska where satellite products typically have large errors in estimating snowfall, especially over snow and ice surfaces (Huffman et al. 2020).

In lack of quality observation of snowfall, it would be useful to utilize other high quality observational products such as SWE, when and where possible. For broader coverage, one has to rely on satellite based SWE observations outside the SNOTEL sites. Two popular operational satellite products for SWE are GlobSnow-2 and AMSR-E/AMSR2. While it has been found that AMSR products are not accurate for SWE estimation (Dawson et al. 2018), GlobSnow-2 seems to provide reasonable estimate of SWE (Luojus et al., 2014a) for non-mountainous regions of the Northern Hemisphere. It goes back to 1979 by integrating in situ data with passive microwave radiometer data from various satellite instruments at daily, weekly, and monthly timescales.

Preprints (www.preprints.org) | NOT PEER-REVIEWED | Posted: 2 June 2021 doi:10.20944/preprints202106.0062.v1

Figure *6* compares SWE accumulation peak from GlobSnow (Figure *6*) and AMSR-2 (Figure *6*) with the corresponding SNOTEL-SWE used in this study. GlobSnow and AMSR-2 do not use the SNOTEL data. GlobSnow shows fairly good correlation with SNOTEL-SWE (CC=0.72) with low bias, defined as the ratio of snowfall accumulation from GlobSnow over snow accumulation at SNOTEL-SWE (no bias is represented by 1). On the other hand, AMSR-2 shows low correlation, high RMSE, and significant underestimation compared to SNOTEL-SWE. The higher skill of GlobSnow compared to AMSR-2 is consistent with previous studies (Hancock et al., 2013; Schroeder et al., 2019; J. W. Yang et al., 2020) and suggests that GlobSnow is more appropriate than AMSR-2 for SWE estimation. However, GlobSnow has no coverage over mountainous regions that is a limiting factor. In addition, GlobSnow may underestimate deep snow (or high SWE; Luojus et al., 2014b) and overestimate shallow snow (or low SWE) as can be seen in Figure *6*.

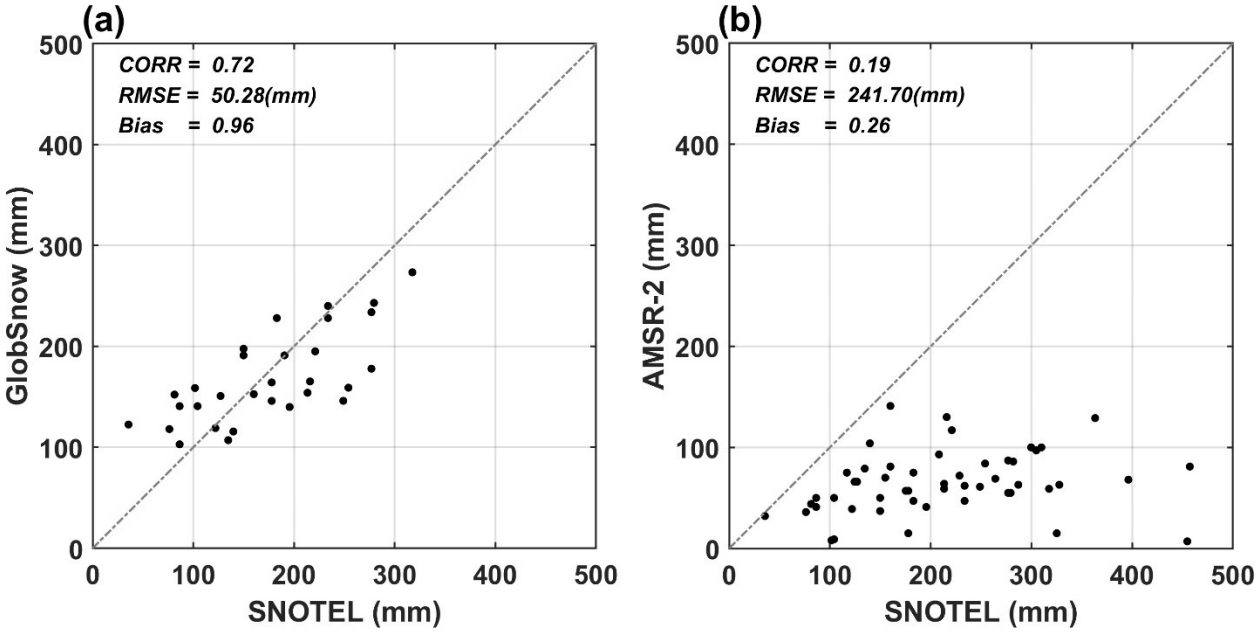

Figure 6. Comparison of SWE estimates between SNOTEL and (a) GlobSnow, and (b) AMSR-2 for water years 2018 and 2019.

For the deep snow cases and for observations over mountains, a potential alternative could be the use of Sentinel-1 snow depth product that has shown good skill in capturing deep snow over mountains (Lievens et al., 2019), although this one has to deal with uncertainties in converting snow depth to SWE. Figure *7* shows an example of comparing snow depth during the snow accumulation phase from two SNOTEL sites (shown in rows) with that from Sentinel-1, GlobSnow, and AMSR-2 at a range of spatial resolutions from 0.25° (corresponding to GlobSnow and AMSR-2) to 1 km offered by Sntinel-1 snow depth (Lievens et al., 2019). Snow depth from AMSR-E and GlobSnow is calculated using snow density determined at SNOTEL sites by dividing the measured snow depth by the measured SWE. Figure *7* shows that GlobSnow and Sentinel-1 are able to capture SNOTEL snow depth much better than AMSR-2, although GlobSnow tends to

Preprints (www.preprints.org) | NOT PEER-REVIEWED | Posted: 2 June 2021 doi:10.20944/preprints202106.0062.v1

overestimate, and Sentinel-1 tends to underestimate the SNOTEL snow depth. Moving from 0.25° to 1 km resolution, Sentinel-1 shows a better match with SNOTEL near the peak of snow depth. The high spatial resolution of Sentinel is valuable, because the estimates can be used at various spatial scales and can be compared with other products. In fact, by comparing coincident snow depth observations from Sentinel-1 and SNOTEL, Figure *8* shows a better overall statistic for Sentinel with original resolution (i.e., 1 km) than a coarser resolution Sentinel at 0.1° and 0.25°. However, it is important to note that Sentinel-1 observations are not available every day and the frequency of observation depends on location and overpass times, varying between daily and once every two weeks. This is the reason why in Figure *7* Sentinel-1 has a lower frequency of sampling compared to GlobSnow and AMSR-2 that provide daily estimates. Nonetheless, combination of GlobSnow and Sentinel observations provide opportunities to further assess snow accumulations over broad regions including mountains. Such observations together with snowfall estimates from space can provide complementary information for further assessment of snow accumulation and monitoring snowpack that is critical for water resources. For all of these estimates accurate quantification of errors can help determine which product and at what location and time might be more trusted for providing snowfall-related information, so individual or combination of the products can be used more effectively.

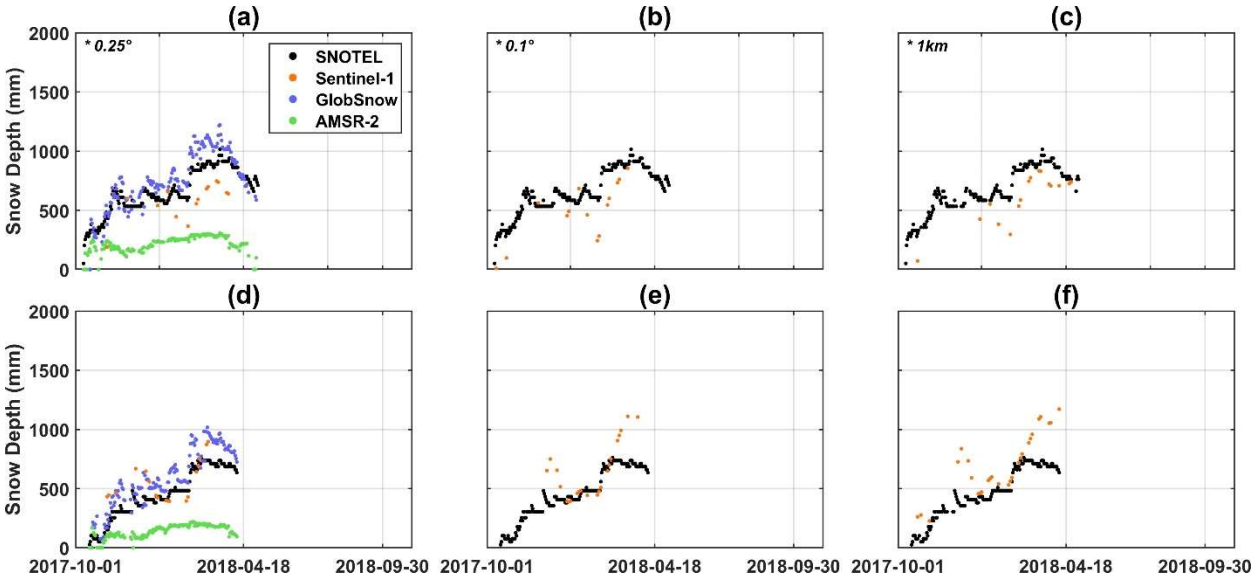

Figure 7. Comparing snow depth during the snow accumulation phase from two SNOTEL sites (shown in rows) with that from Sentinel-1, GlobSnow, and AMSR-2 at a range of spatial resolutions from 0.25 ° (corresponding to GlobSnow and AMSR-2) to 1km from Sntinel-1 snow depth product for water year 2018.

Preprints (www.preprints.org) | NOT PEER-REVIEWED | Posted: 2 June 2021 doi:10.20944/preprints202106.0062.v1

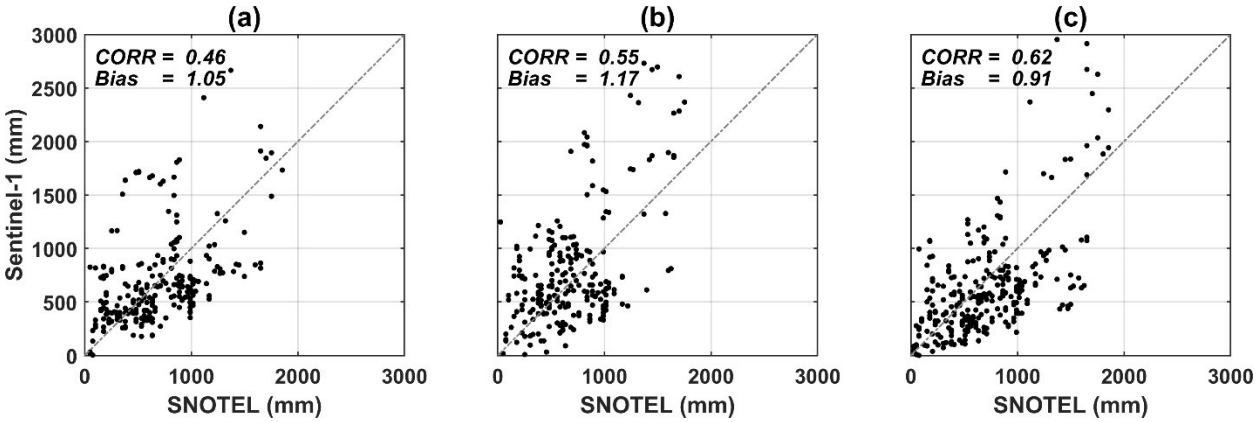

Figure 8. Comparing coincident snow depth observations from Sentinel-1 and SNOTEL in Alaska at various Sentinel-1 resolutions: (a) 0.25 °, (b) 0.1 °, and (c) 1 km for water year 2018.

Concluding Remarks

Accurate estimation of precipitation amount and distribution is important to advance science and applications at regional to global scales. Quantification of precipitation, especially snowfall, has been a major challenge in high latitudes, where in-situ observations are limited, gauge undercatch problems can be severe, and remote sensing products are uncertain.

Here we use combination of SNOTEL observations of daily SWE and snowfall to evaluate not only their own consistency, but also various precipitation products. We found that snowfall estimates based on SWE and precipitation gauge data at SNOTEL sites are consistent. The high resolution Stage IV product, available in Alaska at 4 km, also showed good consistency with SNOTEL observations. Together, these products can provide a range to assess other precipitation products. By comparing Stage IV - 4km with its scaled version at 1-degree resolution, it was found that overall snowfall or precipitation bias is not much affected (Figure *3*), but CC is improved at higher resolution (Figure *4*). By comparing the time series of snowfall and SWE accumulation, it was found that most of the products (except IMERG-HQ) are able to capture snowfall events (e.g., **Error! Reference source not found.**), however differences exist in their accumulation.

By using two years of data (2018-2019; consistent with availability of Stage IV observations over Alaska), snowfall accumulation of the precipitation products was compared near the end of snow accumulation season (i.e., almost at peak SWE) at 39 SNOTEL sites. It was found that correction factors applied to GPCC are effective in improving the undercatch of GPCC gauges, especially for snowfall, with CF-F outperforming CF-L overall (Fig. 5). However, no improvement in correlation is seen when correction factors are applied to GPCC. This is also the case for total precipitation, although GPCC products performed much better in capturing total precipitation than snow accumulation based on the Taylor plots. This can be attributed to better performance of rain gauges in capturing rainfall than snowfall. Overall, GPCP, ERA5, and MERRA2 seem to overestimate snow accumulation, while GPCC (without correction factors) and IMERG-HQ underestimate both snow and precipitation accumulation. The combined passive microwave product, IMERG-HQ, has the largest underestimation for snowfall, but it is able to capture the spatial pattern of snowfall similar to some of the other products. This suggests that the passive microwave products can be

Preprints (www.preprints.org) | NOT PEER-REVIEWED | Posted: 2 June 2021 doi:10.20944/preprints202106.0062.v1

improved substantially through bias correction. By comparison, AIRS (based on satellite IR data) performs acceptably in capturing mean precipitation, but tends to slightly overestimate both total precipitation and snowfall accumulation in most stations.

While this study utilized a combination of SWE and precipitation observations at several SNOTEL sites in Alaska to assess snowfall in the above mentioned precipitation products, the availability of such observations are limited globally. For example, observation networks that include automated measurements of both snow depth and SWE (similar to most SNOTEL stations), are limited to a few regions, such as to the western part of the North America, and primarily in the mountains. Therefore, it would be beneficial to combine remotely sensed estimates of snowfall with large scale SWE monitoring data to generate better estimates of snowfall. Among these products are GlobSnow (although it has gaps over mountains), snow depth from Sentinel-1 that has shown skill for deep snow over mountainous regions,

and other regional products (e.g., ASO or UA SWE). Future improvement in remote sensing of SWE and snow depth as suggested by the recent national academy decadal survey report (NASEM, 2018) together with improved sensors and retrieval algorithms for snowfall estimation should advance our capabilities to more accurately estimate snowfall features and uncertainties.

Acknowledgments

This study was performed mainly in the University of Arizona. Financial support was made available from NASA MEaSUREs (NNH17ZDA001N-MEASURES) and NASA Weather and Atmospheric Dynamics (NNH19ZDA001N-ATDM) grants.

Preprints (www.preprints.org) | NOT PEER-REVIEWED | Posted: 2 June 2021 doi:10.20944/preprints202106.0062.v1

Reference:

Adhikari, A., Ehsani, M. R., Song, Y., & Behrangi, A. (2020). Comparative Assessment of Snowfall Retrieval From Microwave Humidity Sounders Using Machine Learning Methods. *Earth and Space Science*, *7*(11), e2020EA001357. https://doi.org/https://doi.org/10.1029/2020EA001357

Adler, R. F., Huffman, G. J., Chang, A., Ferraro, R., Xie, P.-P., Janowiak, J., et al. (2003). The Version-2 Global Precipitation Climatology Project (GPCP) Monthly Precipitation Analysis (1979–Present). *Journal of Hydrometeorology*, *4*(6), 1147–1167. https://doi.org/10.1175/1525-7541(2003)004<1147:TVGPCP>2.0.CO;2

Adler, R. F., Gu, G., Sapiano, M., Wang, J.-J., & Huffman, G. J. (2017). Global Precipitation: Means, Variations and Trends During the Satellite Era (1979–2014). *Surveys in Geophysics*, *38*(4), 679–699. https://doi.org/10.1007/s10712-017-9416-4

Arabzadeh, A., Ehsani, M. R., Guan, B., Heflin, S., & Behrangi, A. (2020). Global Intercomparison of Atmospheric Rivers Precipitation in Remote Sensing and Reanalysis Products. Journal of Geophysical Research: Atmospheres, 125(21). https://doi.org/10.1029/2020jd033021

Aumann, H. H., Chahine, M. T., Gautier, C., Goldberg, M. D., Kalnay, E., McMillin, L. M., et al. (2003). AIRS/AMSU/HSB on the aqua mission: Design, science objectives, data products, and processing systems. *IEEE Transactions on Geoscience and Remote Sensing*, *41*(2 PART 1), 253–263. https://doi.org/10.1109/TGRS.2002.808356

Barnett, T. P., Adam, J. C., & Lettenmaier, D. P. (2005, November 17). Potential impacts of a warming climate on water availability in snow-dominated regions. *Nature*. Nature Publishing Group. https://doi.org/10.1038/nature04141

Becker, A., Finger, P., Meyer-Christoffer, A., Rudolf, B., Schamm, K., Schneider, U., & Ziese, M. (2013). A description of the global land-surface precipitation data products of the Global Precipitation Climatology Centre with sample applications including centennial (trend) analysis from 1901-present. *Earth System Science Data*, *5*(1), 71–99. https://doi.org/10.5194/essd-5-71-2013

Behrangi, A., Stephens, G., Adler, R. F., Huffman, G. J., Lambrigtsen, B., & Lebsock, M. (2014). An Update on the Oceanic Precipitation Rate and Its Zonal Distribution in Light of Advanced Observations from Space. *Journal of Climate*, *27*(11), 3957–3965. https://doi.org/10.1175/JCLI-D-13-00679.1

Behrangi, A., Andreadis, K., Fisher, J. B., Turk, F. J., Granger, S., Painter, T., & Das, N. (2014). Satellite-Based Precipitation Estimation and Its Application for Streamflow Prediction over Mountainous Western U.S. Basins. *Journal of Applied Meteorology and Climatology*, *53*(12), 2823–2842. https://doi.org/10.1175/JAMC-D-14-0056.1

Behrangi, A., Tian, Y., Lambrigtsen, B. H., & Stephens, G. L. (2014). What does CloudSat reveal about global land precipitation detection by other spaceborne sensors? *Water Resources Research*, *50*(6), 4893–4905. https://doi.org/10.1002/2013WR014566

Behrangi, A., Gardner, A., Reager, J. T., Fisher, J. B., Yang, D., Huffman, G. J., & Adler, R. F.

Preprints (www.preprints.org) | NOT PEER-REVIEWED | Posted: 2 June 2021 doi:10.20944/preprints202106.0062.v1

(2018). Using GRACE to Estitmate Snowfall Accumulation and Assess Gauge Undercatch Corrections in High Latitudes. *Journal of Climate*, *31*(21), 8689–8704. https://doi.org/10.1175/JCLI-D-18-0163.1

Behrangi, A., Singh, A., Song, Y., & Panahi, M. (2019). Assessing Gauge Undercatch Correction in Arctic Basins in Light of GRACE Observations. *Geophysical Research Letters*, *46*(20), 11358–11366. https://doi.org/https://doi.org/10.1029/2019GL084221

Broxton, P. D., N. Dawson, and X. Zeng (2016), Linking snowfall and snow accumulation to generate spatial maps of SWE and snow depth, Earth and Space Science, 3(6), 246-256, doi: 10.1002/2016EA000174.

Broxton, P. D., Zeng, X., & Dawson, N. (2016). Why do global reanalyses and land data assimilation products underestimate snow water equivalent? *Journal of Hydrometeorology*, *17*(11), 2743–2761.

Dawson, N., P. Broxton, and X. Zeng (2018), Evaluation of Remotely Sensed Snow Water Equivalent and Snow Cover Extent over the Contiguous United States, Journal of Hydrometeorology, 19(11), 1777-1791, doi: 10.1175/jhm-d-18-0007.1.

Ehsani, M. R., Behrangi, A., Adhikari, A., Song, Y., Huffman, G. J., Adler, R. F., Bolvin, D. T., & Nelkin, E. J. (2021). Assessment of the Advanced Very High Resolution Radiometer (AVHRR) for Snowfall Retrieval in High Latitudes Using CloudSat and Machine Learning, Journal of Hydrometeorology, 22(6), 1591-1608. Retrieved Jun 4, 2021, from https://journals.ametsoc.org/view/journals/hydr/22/6/JHM-D-20-0240.1.xml

Fuchs, T., Rapp, J., Rubel, F., & Rudolf, B. (2001). Correction of synoptic precipitation observations due to systematic measuring errors with special regard to precipitation phases. *Physics and Chemistry of the Earth, Part B: Hydrology, Oceans and Atmosphere*, *26*(9), 689–693. https://doi.org/10.1016/S1464-1909(01)00070-3

Gelaro, R., McCarty, W., Suárez, M. J., Todling, R., Molod, A., Takacs, L., et al. (2017). The Modern-Era Retrospective Analysis for Research and Applications, Version 2 (MERRA-2). *Journal of Climate*, *30*(14), 5419–5454. https://doi.org/10.1175/JCLI-D-16-0758.1

Gonzalez, R., & Kummerow, C. D. (2020). AMSR-E Snow: Can Snowfall Help Improve SWE Estimates? *Journal of Hydrometeorology*, *21*(11), 2551–2564.

Goodison, B. E., Louie, P. Y. T., & Yang, D. (1998). WMO solid precipitation measurement intercomparison.

Hancock, S., Baxter, R., Evans, J., & Huntley, B. (2013). Evaluating global snow water equivalent products for testing land surface models. *Remote Sensing of Environment*, *128*, 107–117. https://doi.org/https://doi.org/10.1016/j.rse.2012.10.004

Hersbach, H. (2016). The ERA5 Atmospheric Reanalysis. In *AGU Fall Meeting Abstracts*.

Huffman, G. J., Adler, R. F., Morrissey, M. M., Bolvin, D. T., Curtis, S., Joyce, R., et al. (2001). Global Precipitation at One-Degree Daily Resolution from Multisatellite Observations. *Journal of Hydrometeorology*, *2*(1), 36–50. https://doi.org/10.1175/1525-7541(2001)002<0036:GPAODD>2.0.CO;2

Preprints (www.preprints.org) | NOT PEER-REVIEWED | Posted: 2 June 2021 doi:10.20944/preprints202106.0062.v1

Huffman, G. J., Adler, R. F., Bolvin, D. T., & Gu, G. (2009). Improving the global precipitation record: GPCP Version 2.1. *Geophysical Research Letters*, *36*(17). https://doi.org/10.1029/2009GL040000

Huffman, G. J., Bolvin, D. T., Braithwaite, D., Hsu, K. L., Joyce, R. J., Kidd, C., et al. (2020). Integrated Multi-satellite Retrievals for the Global Precipitation Measurement (GPM) Mission (IMERG). In *Advances in Global Change Research* (Vol. 67, pp. 343–353). Springer. https://doi.org/10.1007/978-3-030-24568-9_19

Kunkel, K. E., Robinson, D. A., Champion, S., Yin, X., Estilow, T., & Frankson, R. M. (2016, June 1). Trends and Extremes in Northern Hemisphere Snow Characteristics. *Current Climate Change Reports*. Springer. https://doi.org/10.1007/s40641-016-0036-8

Larsen, C. F., Motyka, R. J., Freymueller, J. T., Echelmeyer, K. A., & Ivins, E. R. (2004). Rapid uplift of southern Alaska caused by recent ice loss. *Geophysical Journal International*, *158*(3), 1118–1133.

Legates, D. R., & Willmott, C. J. (1990). Mean seasonal and spatial variability in gauge-corrected, global precipitation. *International Journal of Climatology*, *10*(2), 111–127. https://doi.org/10.1002/joc.3370100202

Levizzani, V., Laviola, S., & Cattani, E. (2011). Detection and measurement of snowfall from space. *Remote Sensing*, *3*(1), 145–166.

Lievens, H., Demuzere, M., Marshall, H., Reichle, R. H., Brucker, L., Brangers, I., et al. (2019). Snow depth variability in the Northern Hemisphere mountains observed from space. *Nature Communications*, 1–12. https://doi.org/10.1038/s41467-019-12566-y

Liu, G. (2008). A Database of Microwave Single-Scattering Properties for Nonspherical Ice Particles. *Bulletin of the American Meteorological Society*, *89*(10), 1563–1570. https://doi.org/10.1175/2008BAMS2486.1

Luojus, K., Pulliainen, J., Takala, M., Lemmetyinen, J., Kangwa, M., Eskelinen, M., et al. (2014). GlobSnow2–Final Report. *Global Snow Monitoring for Climate Research, European Space Agency*.

Luojus, K., Pulliainen, J., Takala, M., Lemmetyinen, J., Smolander, T., & Derksen, C. (2014). The GlobSnow Snow Water Equivalent Product, 22 July 2014. *SnowPEX ISSPI-1, College Park, Maryland, USA*.

National Academies of Sciences, Engineering, and M. (2018). *Thriving on Our Changing Planet: A Decadal Strategy for Earth Observation from Space*. Washington, DC: The National Academies Press. https://doi.org/10.17226/24938

Nelson, B. R., Prat, O. P., Seo, D. J., & Habib, E. (2016). Assessment and implications of NCEP stage IV quantitative precipitation estimates for product intercomparisons. *Weather and Forecasting*, *31*(2), 371–394. https://doi.org/10.1175/WAF-D-14-00112.1

Painter, T. H., Berisford, D. F., Boardman, J. W., Bormann, K. J., Deems, J. S., Gehrke, F., et al. (2016). The Airborne Snow Observatory: Fusion of scanning lidar, imaging spectrometer, and physically-based modeling for mapping snow water equivalent and snow albedo. *Remote Sensing of Environment*, *184*, 139–152.

Preprints (www.preprints.org) | NOT PEER-REVIEWED | Posted: 2 June 2021 doi:10.20944/preprints202106.0062.v1

Panahi, M., & Behrangi, A. (2019). Comparative Analysis of Snowfall Accumulation and Gauge Undercatch Correction Factors from Diverse Data Sets: In Situ, Satellite, and Reanalysis. *Asia-Pacific Journal of Atmospheric Sciences*. https://doi.org/10.1007/s13143-019-00161-6

Schneider, U., Finger, P., Meyer-Christoffer, A., Rustemeier, E., Ziese, M., & Becker, A. (2017). Evaluating the Hydrological Cycle over Land Using the Newly-Corrected Precipitation Climatology from the Global Precipitation Climatology Centre (GPCC). *Atmosphere* . https://doi.org/10.3390/atmos8030052

Schroeder, R., Jacobs, J. M., Cho, E., Olheiser, C. M., DeWeese, M. M., Connelly, B. A., et al. (2019). Comparison of Satellite Passive Microwave With Modeled Snow Water Equivalent Estimates in the Red River of the North Basin. *IEEE Journal of Selected Topics in Applied Earth Observations and Remote Sensing*, *12*(9), 3233–3246. https://doi.org/10.1109/JSTARS.2019.2926058

Skofronick-Jackson, G., Petersen, W. A., Berg, W., Kidd, C., Stocker, E. F., Kirschbaum, D. B., et al. (2017). The Global Precipitation Measurement (GPM) mission for science and society. *Bulletin of the American Meteorological Society*, *98*(8), 1679–1695.

Susskind, J., Piraino, P., Rokke, L., Iredell, L., & Mehta, A. (1997). Characteristics of the TOVS Pathfinder Path A dataset. *Bulletin of the American Meteorological Society*, *78*(7), 1449–1472.

Yang, D., Goodison, B., Metcalfe, J., Louie, P., Elomaa, E., Hanson, C., et al. (2001). Compatibility evaluation of national precipitation gage measurements. *Journal of Geophysical Research: Atmospheres*, *106*(D2), 1481–1491. https://doi.org/https://doi.org/10.1029/2000JD900612

Yang, J. W., Jiang, L. M., Lemmetyinen, J., Luojus, K., Takala, M., Wu, S. L., & Pan, J. M. (2020). Validation of remotely sensed estimates of snow water equivalent using multiple reference datasets from the middle and high latitudes of China. *Journal of Hydrology*, *590*, 125499. https://doi.org/https://doi.org/10.1016/j.jhydrol.2020.125499

Zeng, X., Broxton, P., & Dawson, N. (2018). Snowpack Change From 1982 to 2016 Over Conterminous United States. *Geophysical Research Letters*, *45*(23), 12,940-12,947. https://doi.org/10.1029/2018GL079621